Mon. Not. R. Astron. Soc. **000**, 000–000 (0000) Printed 1 July 2009 (MN LaTeX style file v2.2)

A practical implementation of realistic X-ray transport through an optically thick OB star wind

Maurice A. Leutenegger,[1] Erin M. Martell,[2] James P. MacArthur,[2]
David H. Cohen,[2] Stanley P. Owocki,[3] Marc Gagné[4]
[1] *NASA/Goddard Space Flight Center, Laboratory for High Energy Astrophysics, Code 622, Greenbelt, Maryland 20771, USA*
[2] *Swarthmore College, Department of Physics and Astronomy, Swarthmore, Pennsylvania 19081, USA*
[3] *University of Delaware, Bartol Research Institute, Newark, Delaware 19716, USA*
[4] *West Chester University of Pennsylvania, Department of Geology and Astronomy, West Chester, Pennsylvania 19383, USA*

1 July 2009

ABSTRACT

We present a tabulation of the transmission of a spherically symmetric stellar wind to radiation, in order to model the emergent broad-band soft X-ray emission due to shock-heated plasma distributed throughout the wind. We model the transmission by an exact integration of the formal solution, assuming the emitting plasma and absorbing plasma are mixed at a constant density ratio above some minimum radius, below which there is assumed to be no emission. This model is more realistic than either the slab absorption associated with a corona at the base of the wind or the exospheric approximation that assumes all the emission arises at and above the radius of optical depth unity. By implementing this transmission model in a tabular fashion in the spectral fitting code XSPEC, spectral models that include a realistic treatment of the X-ray transport through the partially optically thick winds of OB stars can be readily calculated and fit to observed X-ray spectra. The transport model can be coupled to a detailed, pre-calculated model of the wavelength-dependent wind opacity, thereby modeling the full spectral energy distribution from a shock-heated stellar wind in the *Chandra* and *XMM-Newton* bandpasses. Preliminary modeling indicates that the X-ray hardness trend of OB stars with spectral subtype can largely be understood as a wind absorption effect.

Key words: stars: mass-loss – stars: winds, outflows – X-rays: stars

1 INTRODUCTION

The absorption of soft X-rays by the powerful, radiation-driven winds of OB stars has long been recognized as a significant effect both on the X-rays observed from these stars and on the physical conditions in their winds. The significant soft X-ray emission observed in OB stars by *Einstein* and *ROSAT* ruled out significant coronal emission as a source of the ubiquitous X-ray emission seen in these massive stars. For this, and other, reasons, wind-shock models for the production of X-rays in OB stars have become accepted, although the details and even some of the basic aspects of these models are still poorly understood. Modeling not only the X-ray emission from OB star winds but also the absorption is crucial for advancing our understanding of the X-ray production mechanisms themselves. Even simply deriving an intrinsic X-ray luminosity for energy budget considerations requires correctly modeling the significant attenuation of the emitting X-rays, especially in the dense winds of O supergiants.

Wind absorption of X-rays may explain the canonical $L_{\rm x}/L_{\rm Bol} \approx 10^{-7}$ law (Owocki & Cohen 1999)

The amount and wavelength dependence of the wind absorption can be used as a diagnostic of the location/distribution of the shock-heated plasma, especially in terms of its effect on individual line profile shapes (Owocki & Cohen 2001)

Because the emitting plasma is spatially distributed throughout the wind, simple prescriptions for the attenuation can be inaccurate. We have developed a method for implementing an exact solution to the radiation transport that can be easily combined with any independent emission model, such as the Astrophysical Plamsa Emission Code (APEC) (Smith et al. 2001) that is widely used in fitting stellar X-ray spectra.

This model can be used to realistically model the low-resolution CCD spectra that are produced in large quantities by surveys of clusters and O associations with *Chandra* and *XMM-Newton*.

And it can be used to model grating spectra in detail, and provides a means of disentangling the wind absorption effects from the emission temperature effects that appear to both contribute to the recently discovered trend in the morphology of OB star spectra observed at high resolution with the *Chandra* gratings (Walborn et al. 2009).

In this paper we...

2 THE RADIATION TRANSPORT MODEL

The transport model is based on Owocki & Cohen (2001). It assumes that the hot, X-ray emitting plasma is mixed smoothly within a cold, spherically symmetric X-ray absorbing wind with a constant ratio of hot to cold wind density above some shock onset radius, R_0. Below that radius, the wind is only cold and X-ray absorbing. This spatial distribution is consistent with the detailed predictions of numerical hydrodynamics simulations of line-driven OB star winds in which the line-driven instability (LDI) (**??**) leads to numerous sites of shock-heated plasma starting at several tenths of a stellar radius above the photosphere (Feldmeier et al. 1997; Runacres & Owocki 2002; **?**). Owocki & Cohen (2001) developed this model to explain the characteristic line profile shapes observed in high-resolution spectra of OB stars, but by ignoring the Doppler shift of the emitting plasma, it can be used to calculate the emergent x-ray flux over the entire *Chandra* bandpass given a specific spectral emission model.

The emergent X-ray luminosity is calculated from

$$L \propto \int_{R_0}^{\infty} \eta e^{-\tau} \mathrm{d}V, \quad (1)$$

where η is the X-ray emissivity (presumably wavelength dependent), τ is the optical depth from the observer to a given point in the wind, and the volume integral is performed over the entire wind above $r = R_0$. The optical depth, τ, is a function of location in the wind (for a spherically symmetric wind, it depends only on the impact parameter, p, and the radial coordinate with respect to the observer, z), given by

$$\tau(p,z) = \int_z^{\infty} \kappa\rho(r')dz' = \tau_* \int_z^{\infty} \frac{\mathrm{R}_*\mathrm{d}z'}{r'^2(1-\mathrm{R}_*/\mathrm{r}')^{\beta}}, \quad (2)$$

where $r \equiv \sqrt{p^2+z^2}$, and is the independent variable that controls the mass density, ρ, via the mass continuity equation, and κ is the wavelength-dependent atomic opacity of the cold portion of the wind. The second equality arises from substituting the beta-velocity law, $v(r) = v_\infty(1-\mathrm{R}_*/\mathrm{r})^{\beta}$, into the general equation for the optical depth, and the constant, τ_*, is given by

$$\tau_* = \frac{\kappa \dot{M}}{4\pi \mathrm{R}_* \mathrm{v}_\infty}. \quad (3)$$

This parameter is a convenient means for characterizing the overall optical depth of the wind.

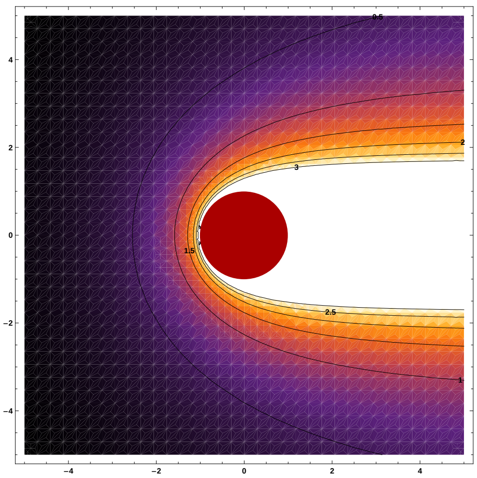

Figure 1. Visualization of the wind emission and absorption model, showing the optical depth as a function of location in the wind for an oberver on the left. The optical depth for the area occulted by the star is infinite.

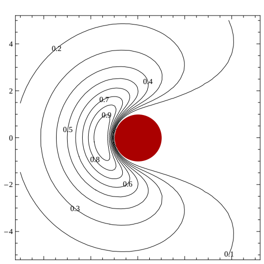

Figure 2. Visualization of the origin of transmitted X-rays. The contours map out a normalization of the function $e^{-\tau(\mu,r)}\rho(r)^2$, a representation of the integrand in Eqn. 1

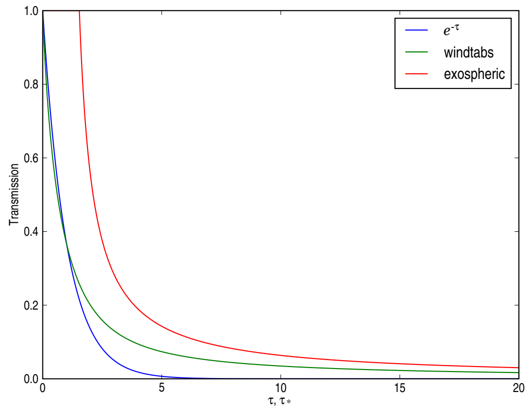

Figure 3. Comparison of the radiation transport model, wintabs, with the exospheric model and a simple slab model. For both all models, $\beta = 1$ and $R_0 = 0.65^{-1}$. In relation to the wintabs model, the slab model provides a reasonable fit for only low τ_*, and the exospheric model exhibits similar end behavior, but neither model is an effective surrogate.

The wind transmission in this model is then given by the ratio of Eqn. 1 to $L(\tau = 0)$. Though fundamentally a function of τ_*, the transmission's wavelength dependence becomes explicit when a wavelength-dependent opacity, $\kappa(\lambda)$ is specified.

Other models of the transmission - slab, exospheric.

3 THE WIND OPACITY MODEL

The nature of the continuum opacity in OB star winds.

Opacity models...

The *windtabs* model makes for a more gradual decrease in transmission with optical depth.

4 MODEL IMPLEMENTATION

Tabular nature of the model, free parameters (R_0, τ_* or $R_0 N_w$?), modular opacity tabulation read in...

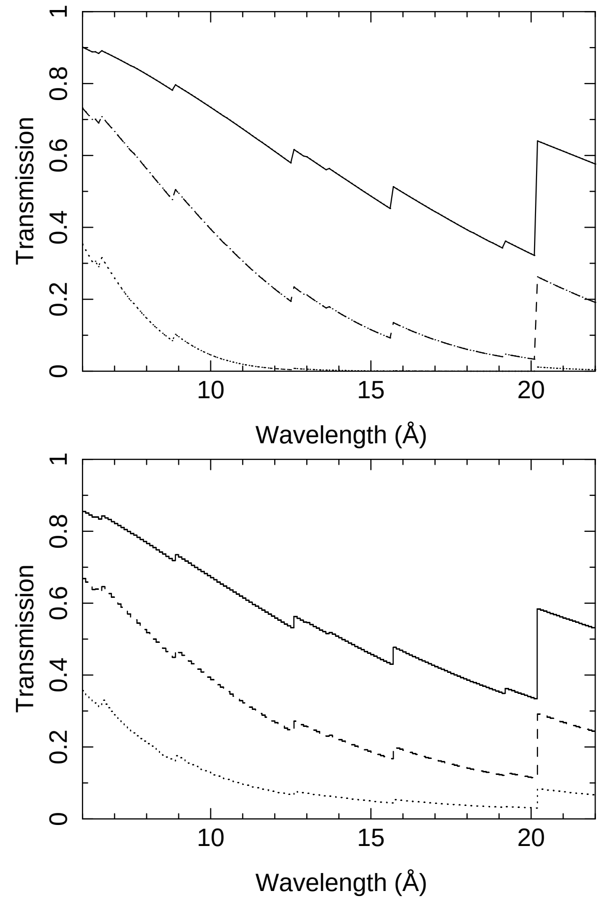

Figure 4. Models of wind transmission (fraction of generated X-ray emission that is emergent from the wind) assuming canonical $I/I_o = e^{-\tau}$ slab absorption (left) and with the *windtabs* distributed emission model (right). For typical values of the wind terminal velocity, stellar radius, and wavelength-dependent opacity, the three curves in each panel correspond to mass-loss rates of 1, 3, and 10 $\times 10^{-6}$ $M_\odot$ yr^{-1} (top to bottom). The difference between the two panels is in the assumed spatial distribution of the emitting plasma. For the left-hand panel, the emitting plasma is entirely below the absorbing wind, and so the transmission goes as $1 - e^{-\tau}$. But for the models in the right-hand panel, the emitting plasma is smoothly distributed throughout the wind – in other words, it is mixed in with the absorbing medium, which makes the transmission a less steep function of optical depth. Note that the transmission decreases more gradually as one looks to higher mass-loss rates for the *windtabs* models. The transmission also changes more gradually for a given mass-loss rate as one looks toward longer wavelengths (where the atomic opacity is larger). The opacity used in these models is due to photoelectric absorption in the cool component of the wind, based on detailed modeling of the wind ionization with CMFGEN, along with abundance constraints from optical spectra, and the atomic cross sections of Verner and Yakovlev (1995). (**I don't know if we want to include this figure or something like it.**)

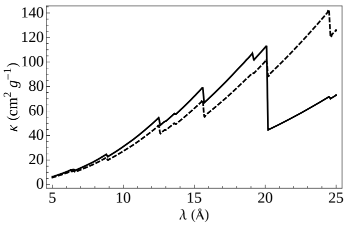

Figure 5. The wind opacity, $\kappa(\lambda)$.

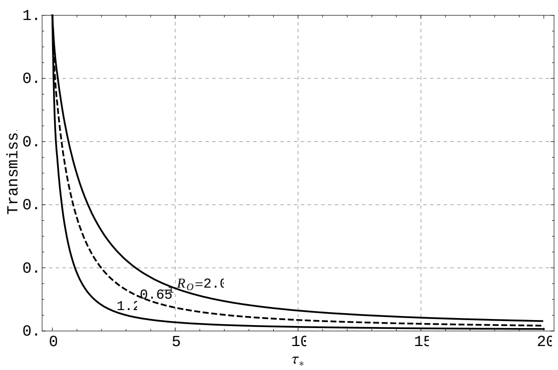

Figure 6. Comparison of wintabs transmission curve for different values of R_0. The variation in transmission for reasonable values of R_0 might merit allowing it to vary???

5 DISCUSSION

superiority of and difference between wintabs to other two models - try fitting some CCD spectrum to compare. ease of use and utility when combined with apec models in xspec - explains the gradual trend shown in last figure.

REFERENCES

Feldmeier A., Puls J., Pauldrach A. W. A., 1997, A&A, 322, 878

Owocki S.P., Cohen D. H., 1999, ApJ, 520, 833

Owocki S.P., Cohen D. H., 2001, ApJ, 559, 1108

Runacres M. C., Owocki S.P., 2002, A&A, 381, 1015

Smith R. K., Brickhouse N. S., Liedahl D. A., Raymond J. C., 2001, ApJ, 556, L91

Walborn N. R., Nichols J. S., Waldron W. L., 2009, ApJ, submitted

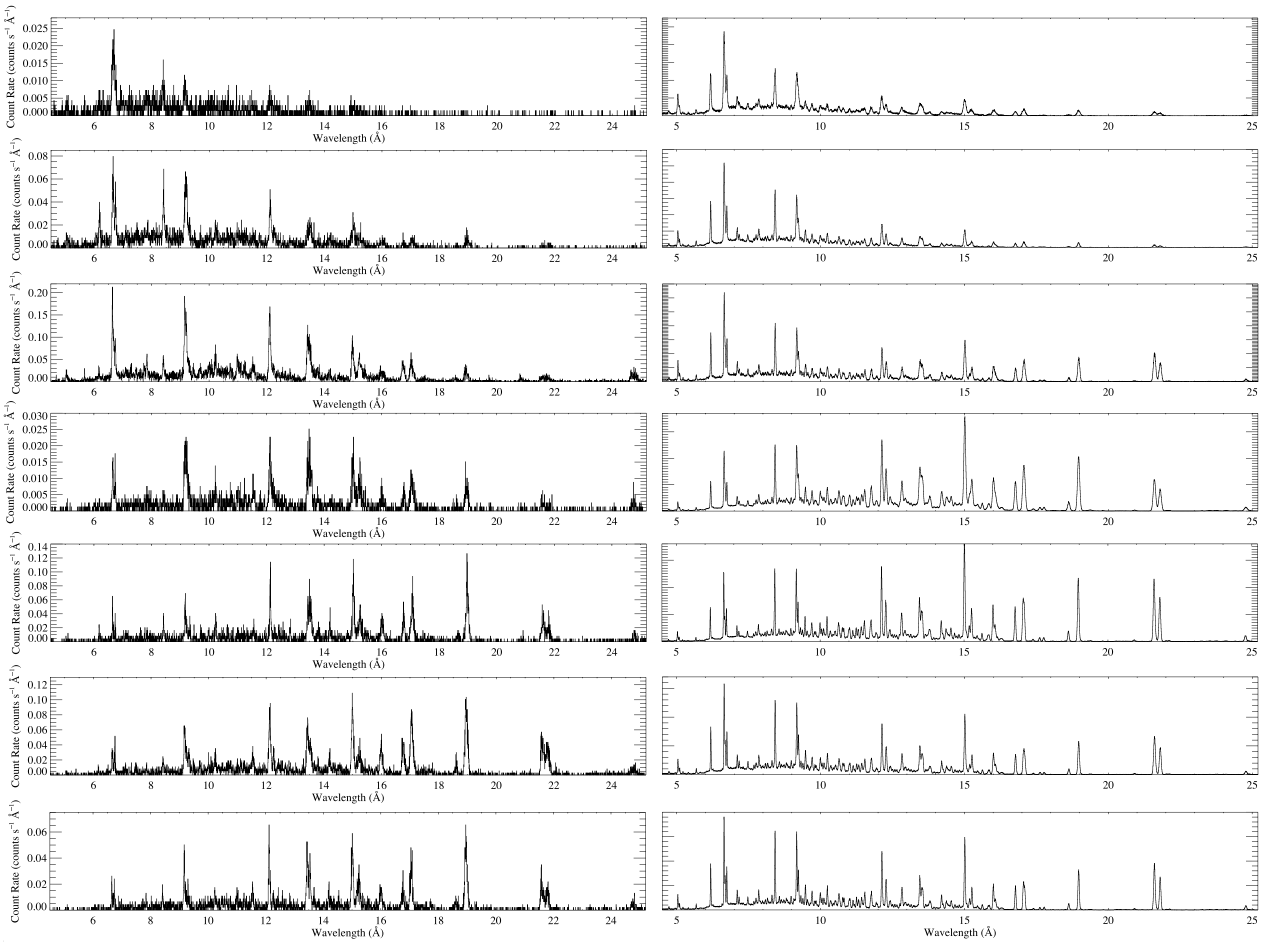

Figure 7. Measured MEG spectra of six O (and one B0) giants and supergiants from the *Chandra* archive (left). From the top, these stars are HD 93129 (O2.5), HD 150136 (O3.5), ζ Pup (O4), ξ Per (O7.5), δ Ori (O9.5), ζ Ori (O9.7), and ϵ Ori (B0). These are the same stars for which Walborn (2006, 2008) identified the hardness trend. In the right-hand panel, we show the same emission model in each panel but combined with the *windtabs* wind absorption model, assuming the literature mass-loss rate for each star.